HETEROCYCLES, Vol. 99, No. 2, 2019, pp. 1154 - 1169. © 2019 The Japan Institute of Heterocyclic Chemistry
Received, 19th September, 2018, Accepted, 14th November, 2018, Published online, 4th February, 2019
DOI: 10.3987/COM-18-S(F)86

PACKING AND THIN-FILM STRUCTURES OF 5,7,12,14-TETRA(α-ALKYLTHIENYLETHYL)PENTACENES

Hiroki Makino, Shin Sato, Junro Yoshino, Naoto Hayashi,* and Hiroyuki Okada*

Graduate School of Science and Engineering, University of Toyama, Gofuku, Toyama 930-8555, Japan. Email: nhayashi@sci.u-toyama.ac.jp, okada@eng.u-toyama.ac.jp

Abstract – Four 5,7,12,14-tetra(thienylethynyl)pentacenes (**2–5**) bearing H, Me, C_5H_{11}, and C_6H_{13} groups at the α-positions of the thienyl groups were synthesized. The α-alkylthienyl groups enhanced solubilities of **2–5**, whereas their ultraviolet/visible spectra were virtually identical. X-Ray diffraction revealed that the packing structure of **4** and **5** were significantly different because of one methylene group in each alkyl group. The thin-film structure of **4** was amorphous, while that of **5** consisted of small crystalline needles. Neither **4** nor **5** behaved as organic field-effect transistors because of inadequate packing and thin-film structure.

INTRODUCTION

Organic field-effect transistors (OFETs) have been examined extensively.[1] Their properties depend on the intrinsic characters of the molecules, especially the π systems, as well as the crystal and thin-film structures. Hence, OFET properties could be refined by modification of the molecular structure, which affects its properties and/or crystal and thin-film structures. With a few exceptions, the intrinsic character of a molecule, such as stability and solubility, can be predicted on the basis of the molecular structure. In contrast, prediction of crystal and thin-film structures based on the molecular structure is quite difficult. Thus, in the design of OFET materials, it is important to understand the relationship between the molecular structure and the crystal and thin-film structures.

Dedicated to Professor Tohru Fukuyama on the occasion of his 70th birthday

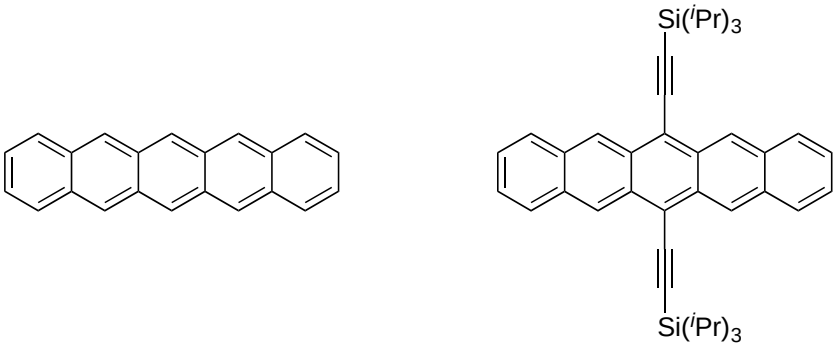

Pentacene TIPS-Pentacene

There are many common modifications of OFET molecules. One of the most important is the introduction of alkynyl groups because they extend the π conjugation system for increased electron-donating and accepting processes and increased intermolecular π-electronic interactions. Furthermore, introduction of the alkynyl group is generally facile. For example, it can be introduced by a combination of nucleophilic substitution of organometallic reagents, followed by reduction,[2] or Sonogashira coupling.[3,4] In OFETs, the most productive alkynyl group is triisopropylsilylethynyl (TIPS).[5] X-Ray structures of 6-(triisopropylsilylethynyl)pentacene and triisopropylsilylethynyl groups (TIPS) have indicated that the pentacenes are forced to arrange in a brick-like manner, which gives rise to two-dimensional intermolecular π interactions. In contrast, the herringbone packing is observed in pentacene itself.

Another important modification is the substitution of heteroaryl groups,[6] which can also extend the π system. In addition, they can increase solubility and enhance intermolecular interactions via hetero atoms. Thienyl groups are the most widely used because they have more electron-donating character and higher chemical stability, and intermolecular contact of sulfur atoms can enhance electronic interactions in OFETs.

In OFETs, pentacene is regarded as the de-facto standard compound, and molecular structure modifications were adopted to pentacene in various ways. There are many pentacene derivatives bearing either alkynyl or heteroaryl groups.

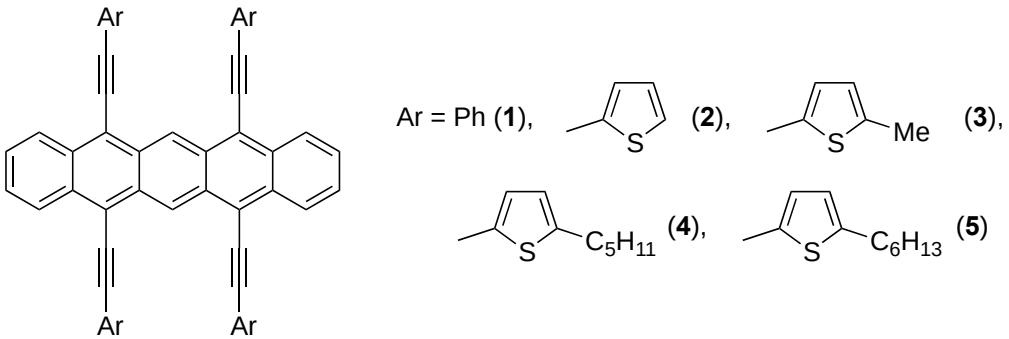

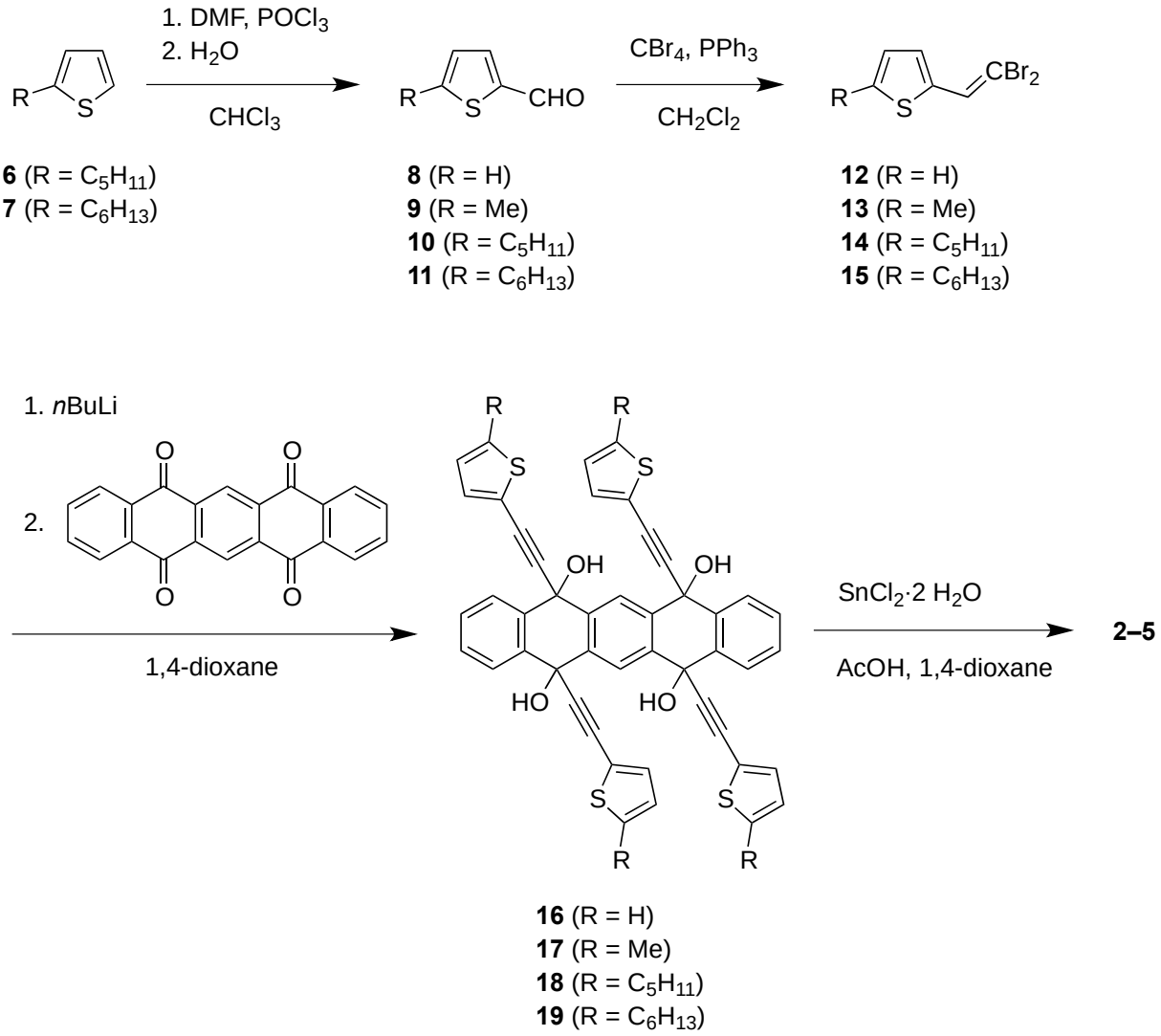

Scheme 1. Synthesis of **2–5**

In contrast, pentacene derivatives bearing heteroarylethynyl groups are rare.[7] Thus, pentacene derivatives bearing theinylethynyl groups at the 5,7,12,14-positions (**2–5**) were synthesized, and their properties, crystal structures, and OFET behaviors were examined relative to their phenylethynyl analogue (**1**).[8] Methyl, pentyl, and hexyl groups were substituted at the α-positions of all thiophene rings in **3**, **4**, and **5**, respectively, to enhance the solubility and to modify the packing structure.

RESULTS AND DISCUSSION

1 was synthesized as before.[8] **2–5** were synthesized from thiophenecarbaldehyde **8–11**, in which **10** and **11** were prepared by the Vilsmeier–Haack reaction[9] of 2-pentyl and 2-hexylthiophenes (**6** and **7**), respectively. **8–11** was subjected to the Corey-Fuchs reaction[10] to give **12–15**, which were converted to alkynyl-lithium by using *n*-BuLi, then reacted with pentacene-5,7,12,14-tetraone to yield tetraols **16–19** as a mixture of stereoisomers.[11] Finally, the tetraols were reduced with tin(II) chloride in acetic acid to

yield **2–5**. The molecular structures were determined by ^{1}H NMR, ^{13}C NMR, mass spectrometry, and infrared spectroscopy; however, ^{13}C NMR spectra of **2**, **3**, **16**, and **17** could not be obtained because of low solubilities.

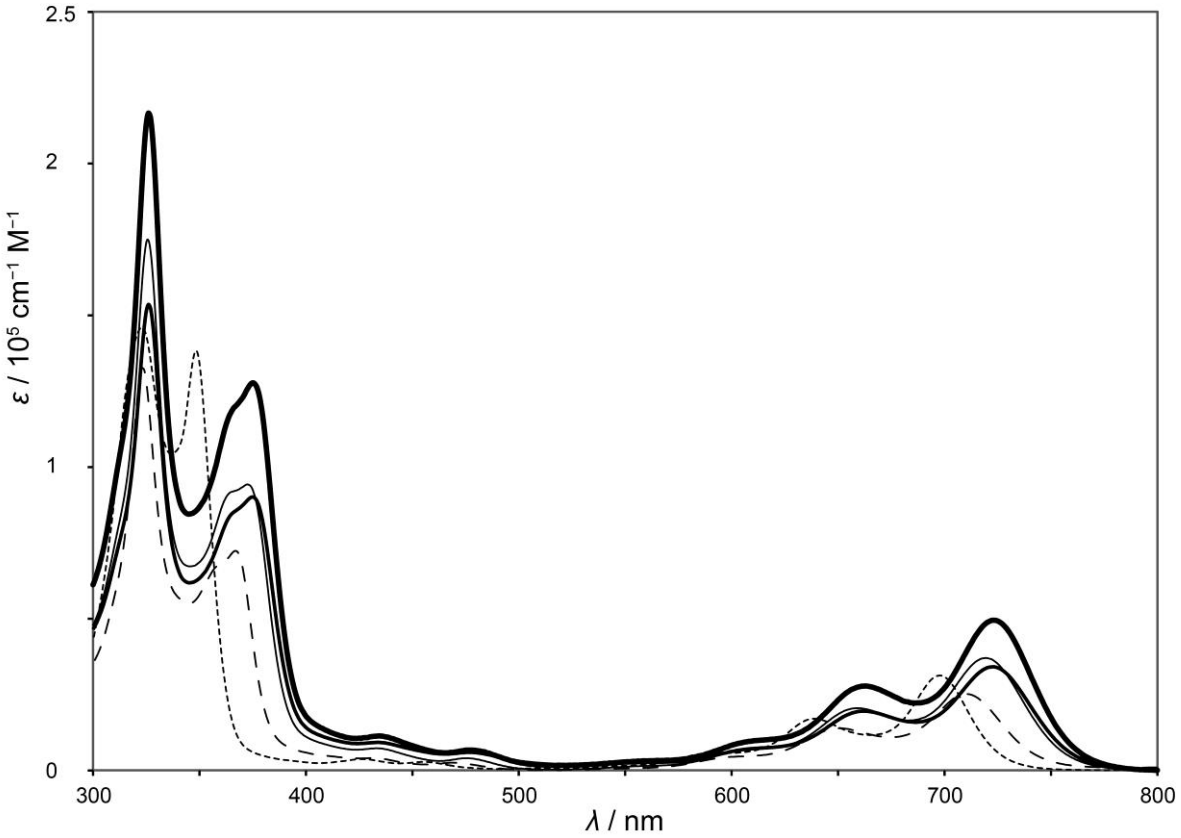

Figure 1. UV/Vis spectra of **1–5** in $CHCl_3$. **1**: thin dotted line, **2**: thin broken line, **3**: thin solid line, **4**: thick solid line, **5**: extra thick solid line

2 was slightly soluble in chloroform and dichloromethane, whereas **1** was even less soluble in those solvents. **2** was unstable and decomposed gradually in these solutions, due to oxidation of the thiophene ring giving thiophen-5-one. In contrast, **3–5** were stable and were more soluble in chloroform and dichloromethane because of the alkyl groups at the α-positions. **4** and **5** were soluble even in chlorobenzene and *o*-dichlorobenzene.

Ultraviolet/visible (UV/Vis) spectra of **1–5** were acquired in chloroform. Pentacene had a longest-wavelength absorption peak λ at 580 nm, while λ for **1–5** were shifted bathochromically to 698–723 nm because of the extended π system from the four arylethynyl groups. The magnitude of the bathochromic shift was in the order **1**<**2**<**3–5**. Bathochromic effects of alkylthienylethnyl groups (in **3–5**) were comparable, and were larger than that of the thienylethynyl group (in **2**).

Density functional theory calculations of **1**, **2**, and pentacene were performed at the B3LYP/6-31G(d,p) level. The highest-occupied molecular orbitals (HOMOs) of **1** and **2** were extended in the pentacene group and in the triple bonds. As a result, the HOMO energy levels E_{HOMO} increased by 0.10 eV (**1**) and 0.12 eV (**2**) relative to that of pentacene. The HOMOs were barely extended to the phenyl and thienyl groups.

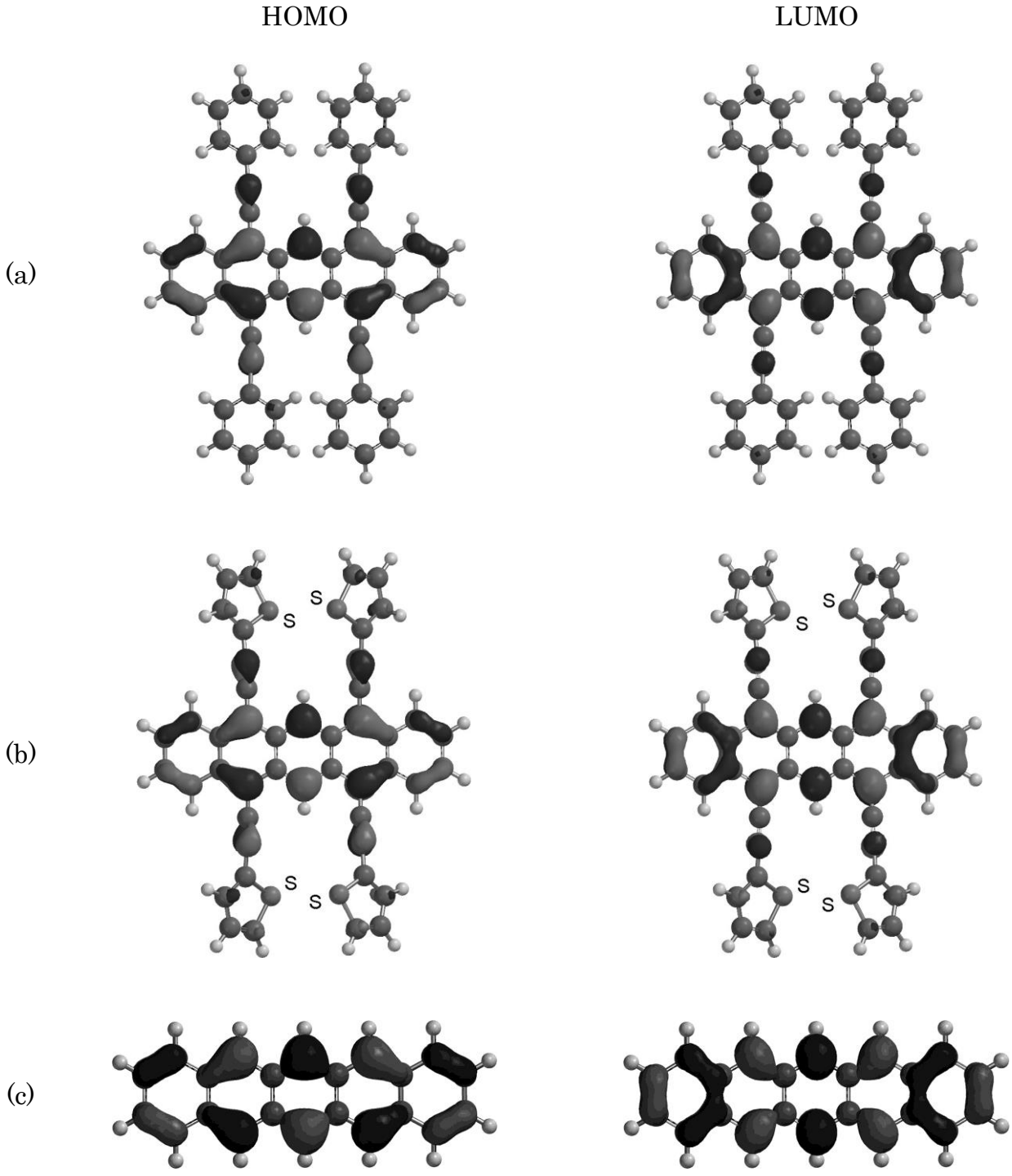

Figure 2. HOMO and LUMO of **1** (a), **2** (b), and pentacene (c)

In contrast, the lowest unoccupied molecular orbitals (LUMOs) of **1** and **2** were extended in pentacene, the triple bonds, and somewhat in the phenyl and thienyl groups. The LUMO energy levels E_{LUMO} were 0.44 eV (**1**) and 0.45 eV (**2**) lower relative to that of pentacene. Consequently, the HOMO–LUMO energy gaps (E_{gap}=E_{LUMO}–E_{HOMO}) of **1** and **2** were significantly decreased to 1.67 eV and 1.64 eV, respectively, which were in agreement with the UV/Vis bathochromic shifts relative to pentacene (E_{gap}=2.25 eV).

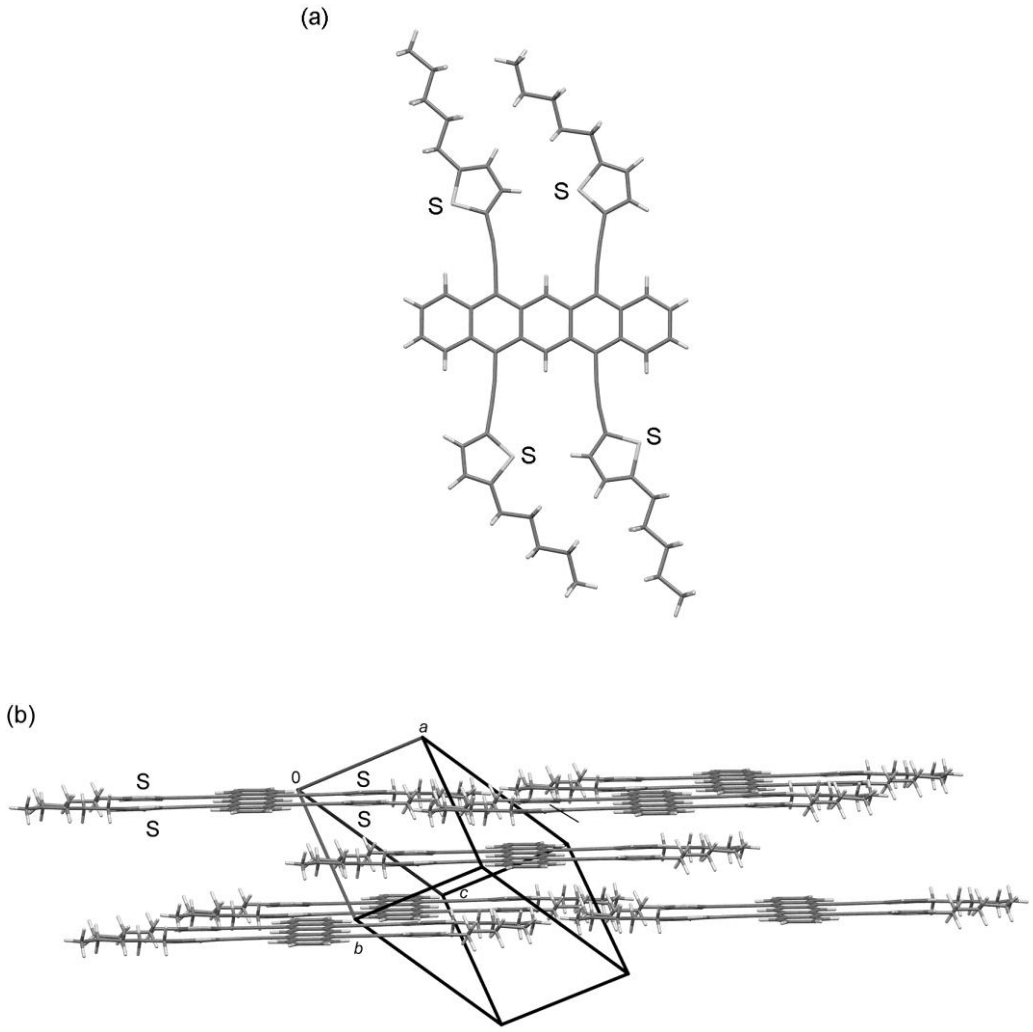

Figure 3. X-Ray structure of **4**. (a) Perspective view of **4**, which was observed to centrosymmetric. (b) Packing structure of **4**

At the energy minima, the phenyl and thienyl groups of **1** and **2** were considerably twisted with respect to the pentacene groups. They had twist angles of 26° for **1** and 34° for **2**, most likely from steric repulsions between adjacent phenyl and thienyl groups.

Because of poor solubilities, single crystal X-ray diffraction data were obtained only for **4** and **5**. During slow evaporation of chloroform, **4** yielded deep-green needles. The X-ray structure revealed a centrosymmetric molecule, where one half of the molecule was crystallographically independent [Figure

3(a)]. The dihedral angles between the pentacene and thienyl moieties were 8.4° and 8.7°, which were smaller than those in the optimized structure from the MO calculation (34° for **2**). The virtually coplanar structure of the π moieties in **4** was probably due to packing. It caused considerable steric repulsion between adjacent thienyl groups, thus giving rise to the slightly bent alkynyl groups. As shown in Figure 3(b), **4** molecules assembled into a brick-like crystalline structure, where the pentacene layers and the thienyl and pentyl layers alternated.

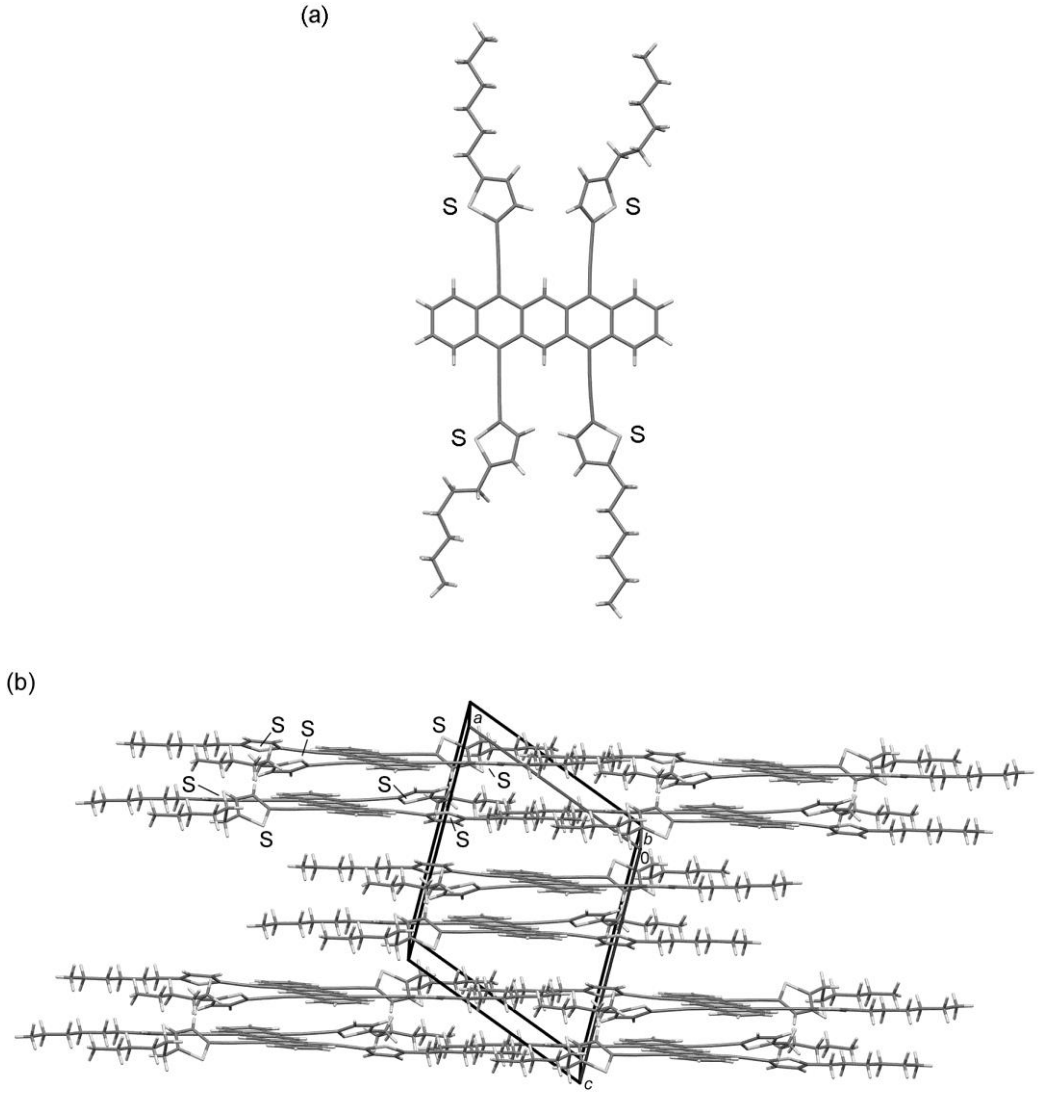

Figure 4. X-Ray structure of **5**. (a) Perspective view of **5**. (b) Packing structure of **5**

MO calculations indicated that the HOMO of **4** was virtually localized on the pentacene groups and the triple bonds; thus, the intermolecular π electronic interaction of the HOMO hardly extended in crystalline **4**. Hence, **4** was not expected to behave as a good p-type semiconductor.

The X-ray crystal structure of **5** was obtained by slow absorption of hexane vapor by an *o*-dichlorobenzene solution. The structure [Figure 4(a)] was quite different from that of **4**. There was one independent **5** molecule. Two of the four thienyl groups adopted a coplanar conformation with respect to the pentacene group (with dihedral angles of 5.3° and 16.3°), while the other two were considerably twisted (24.4° and 41.8°).

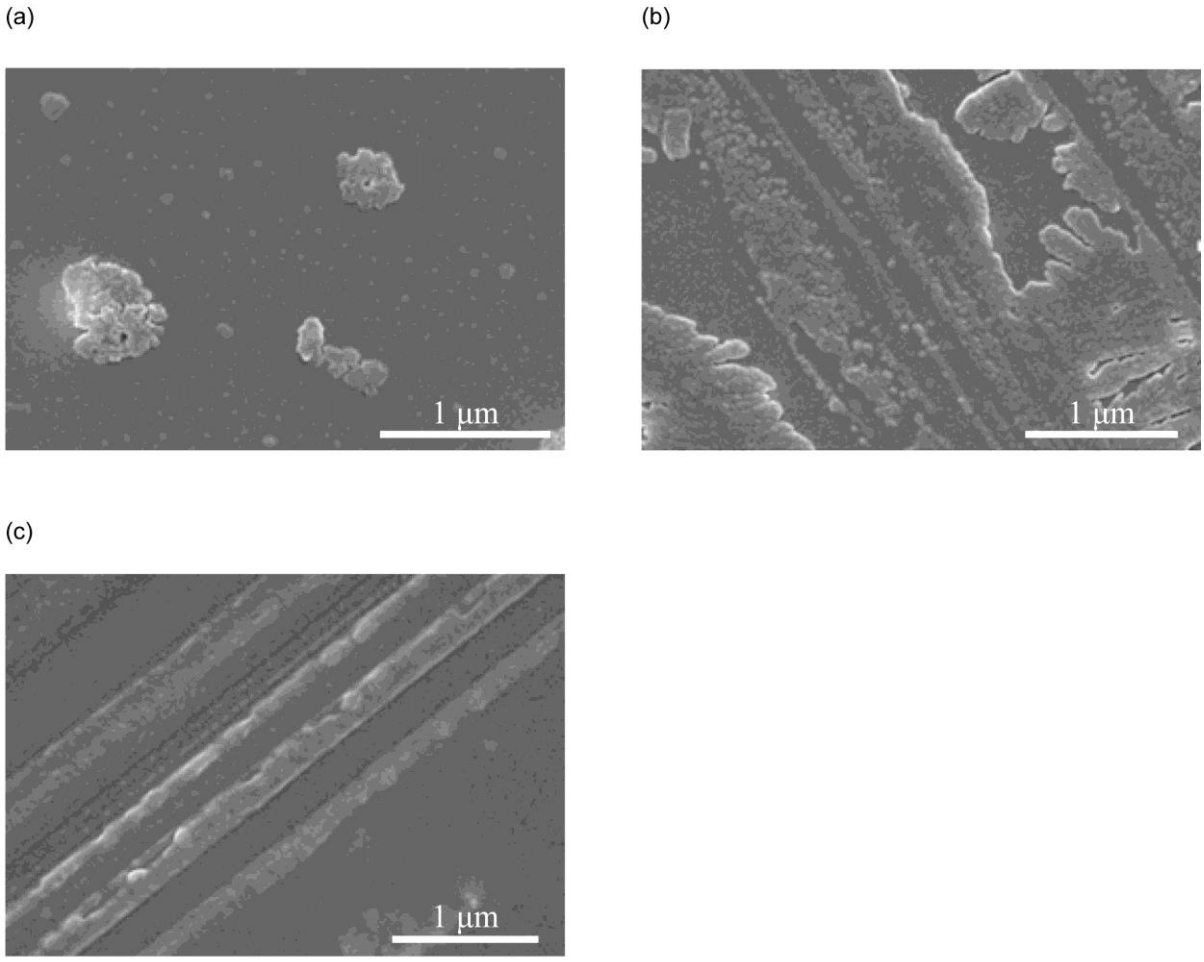

Figure 5. SEM images of **2** (a), **4** (b), and **5** (c)

Consequently, steric repulsion between adjacent thienyl moieties was less in **5** than in **4**, and the alkynyl groups remained linear. As shown in Figure 4(b), two **5** molecules were aggregated by π stacking of pentacene groups in the crystal. The aggregated molecules formed an alternating layer structure parallel to the *bc* plane; layer *a* consisted of pentacene and hexyl groups, while layer *b* consisted of thienyl groups. In layer *a*, the HOMO intermolecular π electronic interaction was restricted within the π-stacked pair because the pair were segregated by hexyl groups. In layer *b*, intermolecular π-stacking of thienyl

moieties was present continuously in a two-dimensional manner, although the HOMO was not virtually extended to the thienyl groups. Thus, **5** was also not expected to behave as a p-type semiconductor.

To examine the effects of alkyl substituents on thin-film structures, thin-films of **2**, **4**, and **5** were prepared by spin coating, and imaged with scanning electron microscopy (SEM).

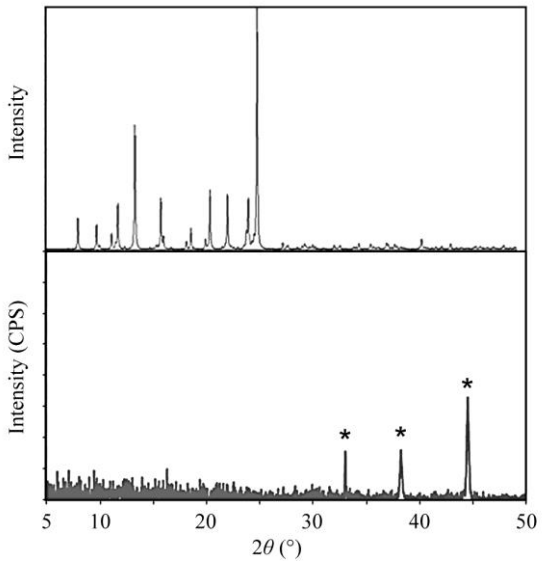

Figure 6. (upper) Simulate XRD pattern of **4** based on the single-crystal X-ray diffraction analysis. (lower) Measured XRD pattern of **4**. Diffraction peaks marked with asterisk are attributed to the silicon substrate.

A SEM image of **2** is shown in Figure 5(a). The thin-film structure was not formed and crystallites were scattered. This was probably because the thin film was prepared from a very dilute solution [0.026% (w/v)] of low-solubility **2**.

In contrast, the thin film of **4** appeared to be homogeneous [Figure 5(b)]. The higher solubility of **4** allowed preparation of the thin-film from a more concentrated solution [0.26% (w/v)]. Unlike that of **2**, no crystallite was found in the SEM image of **4**. Similar SEM images were reported for amorphous thin-films;[12] hence, the thin film of **4** appeared to be amorphous. This was supported by the fact that no Bragg diffraction peak was observed in the X-ray powder diffraction (XRD) pattern of the thin film (Figure 6).

The thin film of **5** was also homogeneous, although it consisted of aligned needle crystallites [Figure 5(c)]. While the molecular structure of **4** was different from that of **5** by only one methylene group per alkyl chain, their thin-film structures were significantly different.

Top-contact OFET devices prepared from spin-coated **4** and **5** were examined. (OFET devices of **1**, **2**, and **3** could not be prepared because of low solubilities). Unfortunately, the **4** and **5** devices did not behave as

p-type OFET devices. This was most likely because of the absence of intermolecular electronic interaction between the HOMOs extending to the whole crystals, and/or because of the poor homogeneity in the thin-film structures. Preparation of OFET devices by vacuum deposition methods was not possible because the compounds decomposed at high temperatures before sublimation.

Conclusively, new pentacene derivates **2–5** bearing thienylethynyl groups at the 5,7,12,14-positions were synthesized, and their solubilities, UV/Vis spectra, X-ray structures, thin-film structures, and OFET behaviors were examined. Compared with the phenyl analogue **1**, the solubility of **2** was enhanced because of substitution of the thienyl group, although **2** was chemically less stable. Stability was improved in **3–5**, which had alkyl substituents at the α-positions of the thienyl groups. Relative to pentacene, significant bathochromic shifts were observed in the UV/Vis spectra for the longest wavelength absorption bands of **1–5**. However, MO calculations revealed that the HOMOs extended to the ethynyl but not to the thienyl groups. When X-ray structures of **4** and **5** were compared, the arrangement of the tetraethynylpentacene groups were significantly different, although their molecular structures differed by only a methylene group in the four alkyl chains. Unfortunately, there was no intermolecular π electronic interaction extending to the whole crystal in **4** and **5**. Consequently, no OFET behavior was observed in their thin-film devices. The amorphous character of the thin films was also responsible for the lack of OFET behavior in **4**.

In the development of functional materials, it is common and useful to change the crystal and thin-film structure by introducing an appropriate alkyl substituent, although prediction of the magnitude of change is still difficult. Further systematic studies on packing and thin-film structures are currently underway.

EXPERIMENTAL

General. $CHCl_3$, CH_2Cl_2, and *N*,*N*-dimethylformamide (DMF) were dried over calcium hydride and distilled over calcium hydride. 1,4-Dioxane was dried over sodium and distilled from sodium containing benzophenone to form the ketyl before use. All other commercially available chemicals were used without further purification. Melting points were determined on microscopic thermometer without correction. ^1H and ^{13}C NMR spectra were recorded on a JEOL ECX-300/TRH (300 MHz for ^1H and 76 MHz for ^{13}C) in $CDCl_3$ unless otherwise mentioned with tetramethylsilane as internal reference. Mass spectra were conducted on a JEOL MStation JMS-700 (EI, FAB, HRMS/EI and HRMS/FAB). Infrared spectra were measured on a JASCO FT/IR-6100 in Nujol mulls. UV/Vis spectra were recorded on a SHIMADZU UV-2400PC spectrometer. Thin-film X-ray diffraction study was performed on a Rigaku ATX-G. Thin-film SEM analysis was conducted on a JEOL-6700F.

Synthesis of 5-pentylthiophene-2-carbaldehyde (10). To a three-necked flask equipped with stirrer and reflux condenser, a solution of 2-pentylthiophene (**6**) (4.65 mL, 28.6 mmol) in DMF (2.5 mL, 31.8 mmol) and $CHCl_3$ (6.5 mL) was added under N_2 atmosphere then stirred at 0 °C. After phosphoryl chloride (2.9 mL, 31.8 mmol) was added dropwisely, the reaction mixture was allowed to room temperature, then refluxed for 4 h. After cooling, water was added, and organic substrate was extracted by using $CHCl_3$. The organic layer was dried over anhydrous $MgSO_4$, and then concentrated to yield **13** as a brown oil (4.74 g, 91%).

^{1}H NMR: δ = 9.82 (s, 1H, CHO), 7.61 (d, *J* = 3.9 Hz, 1H, Ar), 6.90 (dd, *J* = 3.9, 1.2 Hz, Ar), 2.87 (t, *J* = 7.5 Hz, 2H, ArC*H*$_2$), 1.71 (tt, *J* = 7.2, 7.2 Hz, 2H, ArCH$_2$C*H*$_2$), 1.40–1.29 (m, 4H, C*H*$_2$C*H*$_2$CH$_3$), 0.93–0.88 (t, 3H, CH$_3$). MS: *m*/*z* = 182 (M^+).

5-Hexylthiophene-2-carbaldehyde (**11**) was obtained from 2-hexylthiophene (**7**) in a similar manner as a brown oil. Yield 99%. ^{1}H NMR: δ = 9.82 (s, 1H, CHO), 7.61 (d, *J* = 3.9 Hz, 1H, Ar), 6.89 (dd, *J* = 3.6, 0.6 Hz, Ar), 2.87 (t, *J* = 7.5 Hz, 2H, ArC*H*$_2$), 1.71 (tt, *J* = 7.5, 7.5 Hz, 2H, ArCH$_2$C*H*$_2$), 1.39–1.28 (m, 6H, C*H*$_2$C*H*$_2$C*H*$_2$CH$_3$), 0.91–0.87 (t, 3H, CH$_3$). MS: *m*/*z* = 196 (M^+).

Synthesis of 2-(2,2-dibromovinyl)thiophene (12). To a four-necked flask equipped with stirrer, 2-thiophenecarbaldehyde (**8**) (0.85 mL, 9.24 mmol) and CH_2Cl_2 (100 mL) were added under N_2 atmosphere, then stirred at 0 °C. Triphenylphosphine (14.0 g, 53.5 mmol) and carbon tetrabromide (8.93 mg, 26.9 mmol) were added. After stirring for 2 h, the reaction mixture was washed by aqueous sodium bisulfate. The organic layer was dried over anhydrous $MgSO_4$, then concentrated to give yellow oil. The crude product was purified by silica gel column chromatography (hexane) to give **7** as a white solid (2.10 g, 86%).

^{1}H NMR (DMSO-d_6): δ = 8.06 (s, 1H, CHBr$_2$), 7.72–7.70 (m, 1H, Ar), 7.45–7.43 (m, 1H, Ar), 7.13 (dd, *J* = 5.1, 3.9 Hz, 1H, Ar). MS: *m*/*z* = 270 ($[M+4]^+$), 268 ($[M+2]^+$), 266 (M^+).

2-(2,2-Dibromovinyl)-5-methylthiophene (**13**)[13] was obtained from 5-methyl-2-thiophenecarbaldehyde (**9**) in a similar manner as a yellow oil. Yield 98%. ^{1}H NMR: δ = 7.54 (s, 1H, CHBr$_2$), 7.03 (d, *J* = 3.6 Hz, 1H, Ar), 6.68 (dt, *J* = 3.6, 1.2 Hz, 1H, Ar), 2.46 (d, *J* = 1.2 Hz, 3H, CH$_3$). MS: *m*/*z* = 284 ($[M+4]^+$), 282 ($[M+2]^+$), 280 (M^+).

2-(2,2-Dibromovinyl)-5-pentylthiophene (**14**) was obtained from 5-pentyl-2-thiophenecarbaldehyde (**10**) as a yellow oil. Yield 78%. ^{1}H NMR: δ = 7.55 (s, 1H, CHBr$_2$), 7.53 (d, *J* = 3.6 Hz, 1H, Ar), 6.68 (dt, *J* = 3.6, 0.9 Hz, 1H, Ar), 2.77 (dt, *J* = 7.8, 0.9 Hz, 2H, ArC*H*$_2$), 1.71 (tt, *J* = 7.2, 7.2 Hz, 2H, ArCH$_2$C*H*$_2$), 1.37–1.29 (m, 4H, C*H*$_2$C*H*$_2$CH$_3$), 0.92–0.88 (t, 3H, CH$_3$). ^{13}C NMR: δ = 148.48, 135.66, 131.27, 130.26,

123.75, 85.19, 31.36, 31.19, 30.32, 22.47, 14.07. MS: *m*/*z* = 340 ($[M+4]^+$), 338 ($[M+2]^+$), 336 (M^+). HRMS (*m*/*z*): 335.9194 (M^+, calcd. 335.9183 for $C_{11}H_{14}Br_2S$).

2-(2,2-Dibromovinyl)-5-hexylthiophene (**15**) was obtained from 5-pentyl-2-thiophenecarbaldehyde (**11**) as a yellow oil. Yield 82%. ^{1}H NMR: δ = 7.55 (s, 1H, $CHBr_2$), 7.55 (d, *J* = 3.3 Hz, 1H, Ar), 6.70 (dt, *J* = 3.9, 1.2 Hz, 1H, Ar), 2.78 (dt, *J* = 7.5, 1.2 Hz, 2H, ArCH_2) , 1.68 (tt, *J* = 7.2, 7.2 Hz, 2H, $ArCH_2CH_2$), 1.41–1.25 (m, 6H, $CH_2CH_2CH_2CH_3$), 0.91–0.86 (t, 3H, CH_3). ^{13}C NMR: δ = 148.48, 135.66, 131.28, 130.27, 123.75, 85.20, 31.63, 31.48, 30.36, 28.87, 22.65, 14.17. MS: *m*/*z* = 354 ($[M+4]^+$), 352 ($[M+2]^+$), 350 (M^+). HRMS (*m*/*z*): 349.9349 (M^+, calcd. 349.9339 for $C_{12}H_{16}Br_2S$).

Synthesis of 5,7,12,14-tetrakis(2-thienylethynyl)-5,7,12,14-tetrahydropentacene-5,7,12,14-tetraol (16). To a three-necked flask equipped with drop funnel and stirrer, **12** (0.900 g, 3.38 mmol) and 1,4-dioxane (10 mL) were added under N_2 atmosphere, then stirred at 0 °C. To the solution, *n*-butyllithium (1.6 M in *n*-hexane, 4.2 mL, 6.74 mmol) was dropwised via drop funnel during 10 min. After stirring for 1 h, the reaction mixture was allowed to room temperature (solution A). Separately, to a three-necked flask equipped with drop funnel, condenser, and stirrer, pentacene-5,7,12,14-tetraone (0.102 g, 0.301 mmol) and 1,4-dioxane (10 mL) were added under N_2 atmosphere (solution B). To stirred solution B, solution A was added slowly at 0 °C. Afterwards, the reaction mixture was stirred at 100 °C for 12 h. After cooling, aqueous NH_4Cl (0.2 M, 20 mL) was added, and the organic substrate was extracted by EtOAc. The organic layer was condensed mostly, then hexane was added until precipitate appeared. The precipitate was filtered off, washed with hexane, and dried in vacuum. The crude product was purified by silica gel chromatography ($CHCl_3$: EtOAc = 3 : 2) to yield **16** as a brown solid (0.0510 g, 22%).

Mp >300 °C. ^{1}H NMR (DMSO-d_6): δ = 8.60 (s, 2H, Ar), 7.95 (dd, *J* = 6.3, 3.6 Hz, 4H, Ar), 7.50–7.44 (m, 8H, Ar), 7.40 (s, 4H, OH), 6.98 (dd, *J* = 3.3, 0.9 Hz, 4H, Ar), 6.85 (dd, *J* = 5.1, 3.3 Hz, 4H, Ar). IR (cm^{-1}): 3268 (ν_{O-H}), 2228 ($\nu_{C\equiv C}$). MS: *m*/*z* = 772 (M^+). HRMS (*m*/*z*): 772.0900 (M^+, calcd. 772.0870 for $C_{46}H_{28}O_4S_4$).

5,7,12,14-Tetrakis[(5-methylthiophen-2-yl)ethynyl]-5,7,12,14-tetrahydropentacene-5,7,12,14-tetraol (**17**) was obtained from **13** in a similar manner as a brown solid. Yield 26%. Mp >300 °C. ^{1}H NMR: δ = 8.57 (s, 2H, Ar), 7.96 (dd, *J* = 5.8, 3.3 Hz, 4H, Ar), 7.47 (dd, *J* = 5.9, 3.6 Hz, 4H, Ar), 7.27 (s, 4H, OH), 6.80 (d, *J* = 3.3 Hz, 4H, Ar), 6.57 (dd, *J* = 3.3, 0.9 Hz, 4H, Ar), 2.32 (d, *J* = 0.6 Hz, 12H, CH_3). IR (cm^{-1}): 3268 (ν_{O-H}), 2228 ($\nu_{C\equiv C}$). MS: *m*/*z* = 828 (M^+). HRMS (*m*/*z*): 828.1516 (M^+, calcd. 828.1496 for $C_{50}H_{36}O_4S_4$).

5,7,12,14-Tetrakis[(5-pentylthiophen-2-yl)ethynyl]-5,7,12,14-tetrahydropentacene-5,7,12,14-tetraol (**18**) was obtained from **14** as a brown solid. Yield 26%. Mp >300 °C. ^{1}H NMR: δ = 8.84 (s, 2H, Ar), 8.16 (dd, *J* = 5.7, 3.3 Hz, 4H, Ar), 7.43 (dd, *J* = 5.7, 3.3 Hz, 4H, Ar), 6.91 (d, *J* = 3.3 Hz, 4H, Ar), 6.48 (dd, *J* = 3.6, 0.9 Hz, 4H, Ar), 5.17 (br s, 4H, OH), 2.71 (t, *J* = 7.5 Hz, 8H, $ArCH_2$), 1.62 (tt, *J* = 7.5, 7.5 Hz, 8H, $ArCH_2CH_2$), 1.36–1.34 (m, 16H, $CH_2CH_2CH_3$), 0.91–0.88 (m , 12H, CH_3). ^{13}C NMR: δ = 148.56, 139.39, 138.37, 133.31, 129.05, 127.67, 126.04, 124.00, 119.06, 90.30, 84.45, 71.02, 31.38, 31.30, 30.24, 22.49, 14.09. IR (cm^{-1}): 3268 (ν_{O-H}), 2228 ($\nu_{C\equiv C}$). MS: *m*/*z* = 1052 (M^+). HRMS (*m*/*z*): 1052.3982 (M^+, calcd. 1052.4000 for $C_{66}H_{68}O_4S_4$).

5,7,12,14-Tetrakis[(5-pentylthiophen-2-yl)ethynyl]-5,7,12,14-tetrahydropentacene-5,7,12,14-tetraol (**19**) was obtained from **15** as a brown solid. Yield 26%. Mp >300 °C. ^{1}H NMR: δ = 8.68 (s, 2H, Ar), 8.14 (dd, *J* = 5.7, 3.6 Hz, 4H, Ar), 7.40 (dd, *J* = 5.7, 3.6 Hz, 4H, Ar), 6.87 (d, *J* = 3.3 Hz, 4H, Ar), 6.44 (d, *J* = 3.6 Hz, 4H, Ar), 6.14 (br s, 4H, OH), 2.69 (t, *J* = 7.5 Hz, 8H, $ArCH_2$), 1.62 (tt, *J* = 7.5, 7.5 Hz, 8H, $ArCH_2CH_2$) 1.39–1.25 (m, 26H, $CH_2CH_2CH_2CH_3$), 0.92–0.87 (m, 12H, CH_3). ^{13}C NMR: δ = 148.28, 139.25, 138.26, 133.14, 128.75, 127.48, 125.53, 123.76, 118.91, 89.95, 84.43, 70.88, 31.47, 31.39, 30.09, 28.74, 22.48, 13.97. IR (cm^{-1}): 3268 (ν_{O-H}), 2228 ($\nu_{C\equiv C}$). MS: *m*/*z* = 1108 (M^+). HRMS (*m*/*z*): 1108.4643 (M^+, calcd. 1108.4626 for $C_{70}H_{76}O_4S_4$).

Synthesis of 5,7,12,14-tetrakis(2-thienylethynyl)pentacene (2). To a round-bottom flask, **16** (0.0765 g, 0.0993 mmol) and 1,4-dioxane (8 mL) was added then stirred. To this solution, a solution of $SnCl_2 \cdot 2\ H_2O$ (0.112 g, 0.490 mmol) in 50% aqueous acetic acid (1.1 mL) was added dropwisely. Afterwards, the reaction mixture was stirred for 5 h at room temperature. The precipitate was filtered off, washed by water then hexane, and dried in vacuum to yield **2** as a deep green solid (0.0669 g, 97%).

Mp >300 °C. ^{1}H NMR: δ = 10.10 (s, 2H, Ar), 8.59 (dd, *J* = 6.9, 3.6 Hz, 4H, Ar), 7.56 (dd, *J* = 6.9, 3.6 Hz, 4H, Ar), 7.40–7.37 (m, 8H, Ar), 7.02 (dd, *J* = 5.4, 3.6 Hz, 4H, Ar). IR (cm^{-1}): 2178 ($\nu_{C\equiv C}$). MS: *m*/*z* = 702 (M^+). HRMS (*m*/*z*): 702.0586 (M^+, calcd. 702.0604 for $C_{46}H_{22}S_4$).

5,7,12,14-Tetrakis[(5-methylthiophen-2-yl)ethynyl]pentacene (**3**) was obtained from **17** in a similar manner as a deep green solid. Yield 78%. Mp >300 °C. ^{1}H NMR: δ = 10.09 (s, 2H, Ar), 8.58 (dd, *J* = 6.3 3.0 Hz, 4H, Ar), 7.53 (dd, *J* = 6.6, 3.3 Hz, 4H, Ar), 6.69 (dd, *J* = 3.6, 0.9 Hz, 4H, Ar), 2.53 (s, 12H, CH_3). IR (cm^{-1}): 2172 ($\nu_{C\equiv C}$). MS: *m*/*z* = 758 (M^+). HRMS (*m*/*z*): 758.1219 (M^+, calcd. 758.1230 for $C_{50}H_{30}S_4$).

5,7,12,14-Tetrakis[(5-pentylthiophen-2-yl)ethynyl]pentacene (**4**) was obtained from **18** as a deep green solid. Yield 71%. Mp 145–146 °C. ^{1}H NMR: δ = 10.04 (s, 2H, Ar), 8.56 (dd, *J* = 6.3, 3.0 Hz, 4H, Ar), 7.52 (dd, *J* = 6.6, 3.3 Hz, 4H, Ar), 7.25 (d, *J* = 3.3 Hz, 4H, Ar), 6.69 (d, *J* = 3.9 Hz, 4H, Ar), 2.84 (t, *J* = 7.2 Hz, 8H, $ArCH_2$), 1.74 (tt, *J* = 7.2, 7.2 Hz, 8H, $ArCH_2CH_2$), 1.44–1.39 (m, 16H, $CH_2CH_2CH_3$), 097–

0.93 (m, 12H, CH_3). ^{13}C NMR: δ =138.92, 137.52, 129.94, 129.08, 127.86, 127.68, 127.58, 126.77, 124.47, 124.44, 86.36, 85.99, 31.73, 30.51, 29.03, 22.73, 14.20. IR (cm^{-1}): 2172 ($\nu_{C\equiv C}$). MS: *m*/*z* = 982 (M^+). HRMS (*m*/*z*): 982.3734 (M^+, calcd. 982.3734 for $C_{66}H_{62}S_4$).

5,7,12,14-Tetrakis[(5-hexylthiophen-2-yl)ethynyl]pentacene (**5**) was obtained from **19** as a deep green solid. Yield 87%. Mp 141–142 °C. ^1H NMR: δ = 10.05 (s, 2H, Ar), 8.57 (dd, *J* = 6.3, 3.0 Hz, 4H, Ar), 7.52 (dd, *J* = 6.6, 3.3 Hz, 4H, Ar), 7.25 (d, *J* = 3.3 Hz, 4H, Ar), 6.69 (d, *J* = 3.9 Hz, 4H, Ar), 2.84 (t, *J* = 7.2 Hz, 8H, ArCH_2), 1.72 (tt, *J* = 7.2, 7.2 Hz, 8H, ArCH_2CH_2), 1.43–1.35 (m, 24H, $CH_2CH_2CH_2CH_3$), 095–0.90 (m, 12H, CH_3). ^{13}C NMR: δ = 138.54, 137.49, 129.97, 129.00, 127.80, 127.67, 127.29, 126.68, 123.98, 123.95, 86.40, 85.89, 31.39, 31.30, 30.77, 27.27, 22.48, 14.08. IR (cm^{-1}): 2176 ($\nu_{C\equiv C}$). MS: *m*/*z* = 1038 (M^+). HRMS (*m*/*z*): 1038.4355 (M^+, calcd. 1038.4360 for $C_{70}H_{70}S_4$).

Theoretical calculations. Geometry optimizations were conducted with Spartan PC '16 software package on Microsoft Window 10. In all calculations, B3LYP/6-31G** levels were employed and the *C*2*h*, *C*2*h*, and *D*2*h* symmetry were assumed for **1**, **2**, and pentacene, respectively.

Single-crystal X-ray analysis of 4 and 5. Single-crysltal X-ray diffraction study was performed on a Rigaku R-AXIS RAPID IP diffractometer ($\lambda_{Cu,\,K\alpha}$ = 1.54187 Å). Absorption corrections were applied by using the program ABSCOR.[14] The crystal structure was solved by direct methods (SIR2011[15]) and Fourier technique on the Crystal Structure 4.0[16] crystallographic software package. All non-hydrogen atoms were refined with anisotropic parameters. In the analysis of **4**, all hydrogen atoms were found on a differential Fourier map and refined isotropically. In the analysis of **5**, all hydrogen atoms except H65A–H70C were found on a differential Fourier map and refined isotropically, and hydrogen atoms H65A–H70C were placed in the calculated positions with a common temperature factor. Crystallographic data (excluding structure factors) for the structures in this paper have been deposited with the Cambridge Crystallographic Data Centre as supplementary publication. Copies of the data can be obtained, free of charge, on application to CCDC, 12 Union Road, Cambridge CB2 1EZ, UK, (fax: +44-(0)1223-336033 or e-mail: deposit@ccdc.cam.ac.uk).

4. $C_{66}H_{62}S_4$, *MW* = 983.46, triclinic, $P\bar{1}$ (no. 2), *a* = 9.68327(18), *b* = 11.9664(2), *c* = 12.5457(2) Å, α = 78.247(6)°, β = 82.566(6)°, γ = 67.150(5)°, *V* = 1309.51(7) $Å^3$, *Z* = 1, *T* = 173(2) K, D_c = 1.247 g cm^{-3}, *R1* = 0.0566 (*I* > 2 σ(*I*)), *wR2* = 0.1530 (all data). CCDC 1866691.

5. $C_{70}H_{70}S_4$, *MW* = 1039.56, triclinic, $P\bar{1}$ (no. 2), *a* = 13.6440(3), *b* =14.8104(3), *c* = 16.4015(3) Å, α = 114.193(8)°, β = 108.650(8)°, γ = 90.610(6)°, *V* = 2825.7(3) $Å^3$, *Z* = 2, *T* = 173(2) K, D_c = 1.222 g cm^{-3}, *R1* = 0.0443 (*I* > 2 σ(*I*)), *wR2* = 0.1195 (all data). CCDC 1866692.

OFET behavior. A silicon substrate which has 100 nm-thick SiO_2 on highly n-doped Si was rinsed with acetone and 2-propanol and dried. The pentacene derivatives in *o*-dichlorobenzene were spin-coated on the cleaned silicon surfaces at a rotating speed of 500 rpm for 5 sec then 1500 rpm for 60 sec. A 50 nm thick gold source and drain electrode were vapor-deposited onto the polymer thin film. The current-voltage measurement of thin-film transistors was conducted using a semiconductor device analyzer (KEYSIGHT TECHNOLOGIES, B1500A) in air at room temperature.

ACKNOWLEDGEMENTS

This work was supported by JSPS KAKENHI Grant Number JP17K05776.

REFERENCES

1. J. E. Anthony, *Chem. Rev.*, 2006, **106**, 5028.
2. C. D. Sheraw, T. N. Jackson, D. L. Eaton, and J. E. Anthony, *Adv. Mater.*, 2003, **15**, 2009.
3. K. Sonogashira, Y. Tohda, and N. Hagihara, *Tetrahedron Lett.*, 1975, **16**, 4467; R. Chinchilla and C. Nájera, *Chem. Rev.*, 2007, **107**, 874.
4. F. Liu and A. L. Briseno, *Polym. Prepr. (Am. Chem. Soc., Div. Polym. Chem.)*, 2010, **51**, 475.
5. M. M. Payne, S. R. Parkin, J. E. Anthony, C. Kuo, and T. N. Jackson, *J. Am. Chem. Soc.*, 2005, **127**, 4986; S. K. Park, D. A. Mourey, J. I. Han, J. E. Anthony, and T. N. Jackson, *Org. Electron.*, 2009, **10**, 486.
6. Y.-M. Wang, N.-Y. Fu, S.-H. Chan, H.-K. Lee, and H. N. C. Wong, *Tetrahedron*, 2007, **63**, 8586; Q. Miao, X. Chi, S. Xiao, R. Zeis, M. Lefenfeld, T. Siegrist, M. L. Steigerwald, and C. Nuckolls, *J. Am. Chem. Soc.*, 2006, **128**, 1340.
7. J. Guo, D. Liu, J. Zhang, J. Zhang, Q. Miao, and Z. Xie, *Chem. Commun.*, 2015, **51**, 12004; C. J. Lee, J. S. Lim, J. M. Lee, D. H. Choi, G. H. Kim, and G. N. Kim, *Repub. Korean Kongkae Taeho Kongbo*, 2010, KR 2010118253 A 20101105.
8. D. R. Maulding and B. G. Roberts, *J. Org. Chem.*, 1969, **34**, 1734.
9. O. Meth-Cohn and S. P. Stanforth, *Comp. Org. Synth.*, 1991, **2**, 777.
10. E. J. Corey and P. L. Fuchs, *Tetrahedron Lett.*, 1972, **13**, 3769; J. P. Beny, S. N. Dhawan, J. Kagan, and S. Sundlass, *J. Org. Chem.*, 1982, **47**, 2201.
11. I. Kaur, W. Jia, R. P. Kopreski, S. Selvarasah, M. R. Dokmeci, C. Pramanik, N. E. McGruer, and G. P. Miller, *J. Am. Chem. Soc.*, 2008, **130**, 16274.
12. Y. Sun, K. Xiao, Y. Liu, J. Wang, J. Pei, G. Yu, and D. Zhu, *Adv. Funct. Mater.*, 2005, **15**, 818.
13. G. S. Pilzak, K. van Gruijthuijsen, R. H. van Doorn, B. van Lagen, E. J. R. Sudhçlter, and H. Zuilhof, *Chem. Eur. J.*, 2009, **15**, 9085.

14. ABSCOR, Rigaku Corporation, Tokyo, Japan, 1995.
15. M. C. Burla, R. Caliandro, M. Camalli, B. Carrozzini, G. L. Cascarano, C. Giacovazzo, M. Mallamo, A. Mazzone, G. Polidori, and R. Spagna, *J. Appl. Cryst.*, 2012, **45**, 357.
16. Crystal Structure 4.0, "Crystal Structure Analysis Package", Rigaku Corporation, Tokyo, Japan, 2010.